Universidad Carlos III de Madrid

e-Archivo Institutional Repository

This is a postprint version of the following published document:

"Pozuelo, J., Mendicuti, F. & Mattice, W. L. (1995): Intramolecular excimer formation in naphthalene-containing polyesters. Bichromophoric model compounds derived from phthalic, succinic or malonic acid and 2-hydroxynaphthalene or 2-hydroxymethylnaphthalene. *Macromolecular Chemistry and Physics*, 196 (5), pp.: 1779-1790."

DOI: 10.1002/macp.1995.021960532

© WILEY-VCH Verlag GmbH & Co. KGaA, 1995

Intramolecular excimer formation in naphthalene-containing polyesters. Bichromophoric model compounds derived from phthalic, succinic or malonic acid and 2-hydroxynaphthalene or 2-hydroxymethylnaphthalene

Javier Pozuelo, Francisco Mendicuti

Departamento de Química Física, Universidad de Alcalá, Alcalá de Henares, Madrid, Spain

*Wayne L. Mattice**

Institute of Polymer Science, The University of Akron, Akron, Ohio 44325-3909, USA

SUMMARY:

Steady state fluorescence measurements in dilute solutions are performed for bis(2-naphthyl) phthalate, bis(2-naphthylmethyl) phthalate, bis(2-naphthyl) succinate, bis(2-naphthylmethyl) succinate, bis(2-naphthyl) malonate and bis(2-naphthylmethyl) malonate, as models for polyesters containing naphthalene in their rigid units and flexible spacers that impose differences in the types of interactions between successive naphthalene units. The amount of intramolecular excimer in dilute solution depends on the type of flexible spacer, and also whether the compound is derived from 2-naphthol or 2-hydroxymethylnaphthalene. No excimer is detected from the compounds derived from 2-naphthol, but all compounds derived from 2-hydroxymethylnaphthalene showed excimer formation. These results are rationalized with a theoretical analysis of the conformations of the flexible spacers.

Introduction

Many polymers contain an alternating sequence of rigid units and flexible spacers. The rigid units are often derived from compounds that contain aromatic rings. Naphthalene is one of the popular rigid ring systems that has been used for the rigid unit. Since naphthalene is capable of forming an excimer [1], the dependence of the excimer emission in dilute solution provides information about the types of intramolecular interactions of the rigid units allowed by the conformations accessible to the flexible spacer. The experiment provides values of I_D/I_M, which denotes the ratio of the intensity of the emission from the excimer and the monomer (here "monomer" denotes a naphthalene unit that is not interacting with any other naphthalene unit). However, since naphthalene is also capable of the nonradiative self-transfer of singlet excitation energy, the interpretation of I_D/I_M for a polymer may be complicated by the population of an excimer via energy migration [1]. This potential complication can be eliminated by the study of dilute solutions of bichromophoric model compounds of the form N-spacer-N, where N denotes the naphthalene unit. From these experiments, one can deduce how the probability for a sharp reversal (a "hairpin") in the direction of the chain is influenced by the selection of the spacer.

Often the spacers are derived from linear chains, such as short sequences of methylene[2–5] or oxyethylene[2,6] units. Cyclic spacers that contain cyclohexane are also known[7]. Here we examine spacers that contain ester groups, either incorporated into an acyclic unit or as part of a cyclic structure, the terephthalate moiety. We also investigate the consequences of whether the ester group is bonded directly to the naphthalene unit, or whether a methylene group is inserted between the naphthalene and the ester.

Steady state fluorescence measurements in dilute solutions are performed for six bichromophoric diesters prepared from the six combinations of one of three dicarboxylic acids (phthalic, succinic and malonic acids) and one of two alcohols (2-naphthol and 2-hydroxymethylnaphthalene). The structures and abbreviations for bis(2-naphthyl) phthalate, bis(2-naphthylmethyl) phthalate, bis(2-naphthyl) succinate, bis(2-naphthylmethyl) succinate, bis(2-naphthyl) malonate, and bis(2-naphthylmethyl) malonate are depicted in Fig. 1. Fluorescence measurements were used to determine

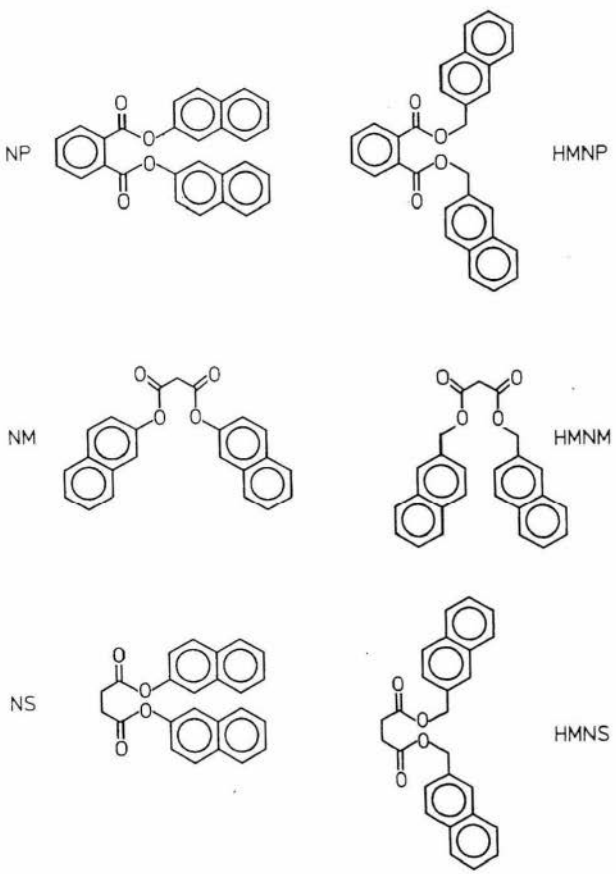

Fig. 1. Structures and abbreviations for the six diesters studied

I_D/I_M in diethyl ether and in several hydrocarbons, in dilute fluid solution. The amount of intramolecular excimer in dilute solution mainly depends on the type of flexible spacer and the solvent. Excimer to monomer intensity ratios I_D/I_M depend strongly on whether the compound is derived from 2-naphthol or 2-hydroxymethylnaphthalene (HMN). They are zero for the three compounds derived from 2-naphthol, but all three compounds derived from HMN showed excimer formation. These latter compounds have two more rotatable bonds in the flexible spacer that do their counterparts derived from 2-naphthol.

A theoretical equilibrium treatment using the Tripos Force Field from Sybyl 6.0, as in recent studies of other systems[7-9], permits the identification of the conformations that are responsible for the types of face-to-face complexes by the overlap of one or two six-membered rings from the different naphthalene units, as well as calculation of the total probability of the conformations conducive to overlap. Notable among these studies was the computational investigation of the same sixteen compounds containing two or three phenyl groups bonded to a short alkane chain that were studied experimentally in the classic work by Hirayama[10]. The calculation correctly separated the nine compounds that formed excimers from the seven compounds that did not[9].

Experimental part

The synthesis was carried out in the same way as previously for related compounds[2-4,7]. In brief, naphthalene groups were attached to the ends of the spacers through the reaction of dichlorides of the diacids with the alcohols containing naphthalene groups. A stoichometry of nearly 1:2 (diacid:alcohol) with a slight excess of the alcohol, in the presence of a 50% excess of triethylamine in purified chloroform[11], was used. The mixture was refluxed for approximately 3 h under an atmosphere of N_2. Once the reaction was completed, the solution was sequentially washed several times with water and aqueous $NaHCO_3$ solution, and finally washed three times with water. This solution was precipitated by concentrating or by adding a small amount of methanol. In all cases, the solid product which precipitated consisted almost totally of the desired disubstituted compound. All of the products were recrystallized twice from a mixture of chloroform and ethanol.

A purity higher than 98% was estimated from the NMR spectra performed in $CDCl_3$ and the ratio of aliphatic and aromatic hydrogens. Reactants and solvents used for the synthesis were purchased from Aldrich. All the solvents for spectrophotometric measurements were spectrophotometric grade, >99% or HPLC grade and, previously checked, they were used without further purification.

Absorption spectra

Absorption spectra were measured at 25 °C with a UV-visible Hewlett Packard 8452A diode array spectrophotometer. Fig. 2 depicts absorption spectra of HMNP and HMN in isopentane at 25 °C. The spectra exhibited a prominent band with two shoulders around it. The band was centered around 276 nm for NP and HMNP, 278 nm for NS and HMNS, and 279 nm for NM and HMNM. Spectra in the other solvents showed similar characteristics.

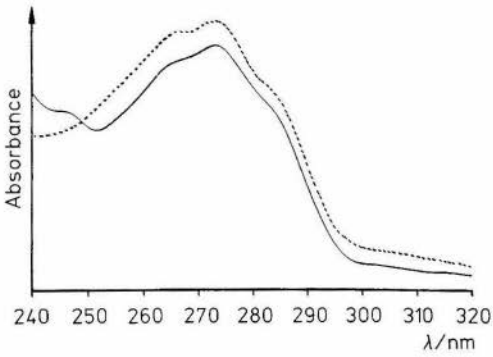

Fig. 2. Absorption spectra for HMN (———) and HMNP (– – –) in isopentane at 25 °C

Fluorescence measurements

Steady state fluorescence measurements were performed with a Perkin Elmer LS-5B fluorimeter, using single monochromators in the excitation and emission paths. Slits were 15 nm for excitation and 2,5 nm for emission. All measurements were performed without polarizers. Solvent baselines were subtracted from each spectrum. Typical absorbances at the wavelength of excitation, 286 nm, were about 0,1. Right angle geometry using rectangular cells with a 1 cm light path was employed for the measurements at 25 °C. Right angle geometry and 2 mm cylindrical cells were used for the measurements at 77 K in isopentane (glassy vitrified solution).

Experimental results

Excitation spectra

Fig. 3 depicts excitation spectra for HMNP, HMNS and HMNM at 77 K in isopentane, using 390 nm for monitoring the emission. These spectra show a band, centered at 276, 278 and 279 nm for HMNP, HMNS and HMNM, respectively, that

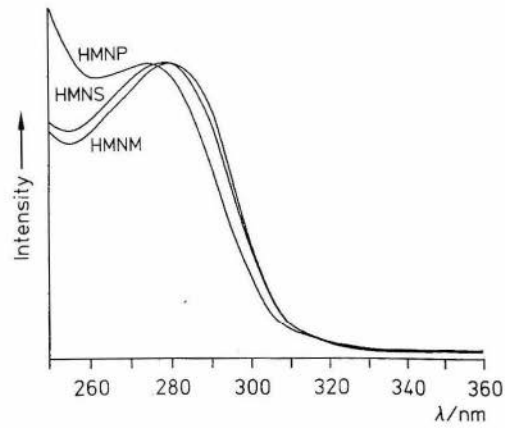

Fig. 3. Excitation spectra for HMNP, HMNS and HMNM in isopentane at 77 K, with the emission monitored at 390 nm

matches very well with the one observed in the absorption spectra. The shape of the excitation spectra does not depend noticeably on the wavelength selected for emission.

Emission spectra

Fig. 4 depicts emission spectra for all six bichromophoric model compounds and HMN as a reference compound in isopentane at 25 °C. Spectra are normalized to the peak of high energy of the emission of HMN (in the range 324–328 nm for the different solvents used). The slight enhancement of the band towards the red observed in three of the six bichromophoric model compounds as compared to the reference compound is attributed to the intramolecular formation of an excimer.

The ratio I_D/I_M was evaluated as[2-4, 7, 8]

$$\frac{I_D}{I_M} = \frac{I_{\text{Bichrom, 390}} - I_{\text{RC, 390}}}{I_{\text{norm}}} \quad (1)$$

where $I_{\text{Bichrom, 390}}$ denotes the normalized fluorescence intensity at 390 nm for the bichromophoric model compounds (390 nm was selected to represent the excimer band). $I_{\text{RC, 390}}$ is the intensity (normalized at 324–328 nm) obtained for the reference compound, HMN or 2-naphthol, at the same wavelength of 390 nm. I_{norm} is the intensity used for normalization of the emission band for the reference compound.

Tab. 1 presents values of I_D/I_M at 25 °C in four of the solvents used for our measurements. No excimer emission is detected for NP, NM or NS. A small amount of excimer is detected for the end-labelled samples derived from the HMN. For these three compounds, the observed trend in the values of I_D/I_M was HMNP > HMNS > HMNM, independent of solvent.

A very low quantum yield for fluorescence for all of the samples when dissolved in alcohols prohibited the manipulation of the viscosity by using (a) a series of *n*-alcohols, (b) mixtures of methanol and ethylene glycol, and (c) ethylene glycol at different tem-

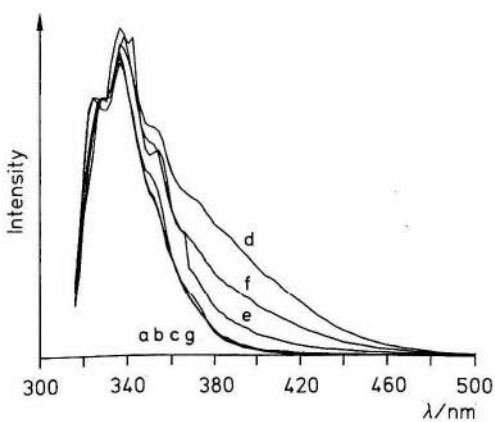

Fig. 4. Emission spectra, normalized at 324–328 nm, for HMN and the six diesters in isopentane at 25 °C. (a) NP, (b) NM, (c) NS, (d) HMNP, (e) HMNM, (f) HMNS and (g) HMN

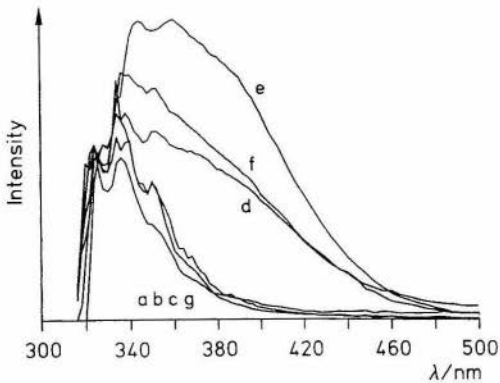

Fig. 5. Emission spectra, normalized at 324 nm, for HMN and the six diesters in isopentane at 77 K. (a) NP, (b) NM, (c) NS, (d) HMNP, (e) HMNM, (f) HMNS and (g) HMN

Tab. 1. The ratio I_D/I_M in four solvents at 25 °C and in isopentane at 77 K

Compound	Diethyl ether	Hexane	Cyclohexane	Isopentane	Isopentane (77 K)
NP, NS, NM	0,00	0,00	0,00	0,00	0,00
HMNP	0,20	0,41	0,42	0,38	0,71
HMNS	0,10	0,17	0,18	0,20	0,78
HMNM	0,03	0,08	0,08	0,07	1,30

peratures. Furthermore, the compounds suffer a degradation in these solvents (the monomer emission band increases, and the excimer band decreases, with time).

Fig. 5 depicts emission spectra for all six bichromophoric model compounds and HMN as a reference compound in isopentane at 77 K upon excitation at 286 nm. Spectra are normalized at 324 nm, the peak of the emission for HMN. Tab. 1 presents the values of I_D/I_M at 77 K in isopentane. Excimers are detected only for the end-labelled samples derived from HMN. For these three compounds the values of I_D/I_M in isopentane are higher at 77 K than at 298 K, and the trend in the value of I_D/I_M was HMNM > HMNS > HMNP. The results show no important influence of dynamics on the formation of the excimers, and they suggest the possibility of excimer dissociation at room temperature, because I_D/I_M is much smaller at this temperature than at 77 K.

Theoretical part

Methodology

The method adopted for the theoretical analysis was similar to the one used previously for related compounds[7-9]. The molecules studied were the diester model compounds depicted in Fig. 1. The first step consists of the generation of the starting conformations. Bond lengths and bond angles for these conformations were obtained

Tab. 2. Parameters for the molecules studied (N_s is defined in Eq. (2), and N_s' and N_c are defined in the two paragraphs following that equation)

Compound	Type of angles (cf. Fig. 6)	Number of bonds	Torsion angle	N_s	N_s'	N_c
NP	θ	2	$\pm 20°$, $\pm 160°$	64	34	306
	μ_1	2	$\pm 90°$			
HMNP	θ	2	$\pm 20°$, $\pm 160°$	576	324	26244
	δ_3	2	$\pm 60°$, $180°$			
	μ_2	2	$\pm 90°$			
NS	δ_1, δ_2	3	$\pm 60°$, $180°$	108	94	22842
	μ_1	2	$\pm 90°$			
HMNS	δ_1, δ_2, δ_3	5	$\pm 60°$, $180°$	972	901 (137)[a]	1970487 (299619)[a]
	μ_2	2	$\pm 90°$			
NM	δ_1	2	$\pm 60°$, $180°$	36	36	2916[a]
	μ_1	2	$\pm 90°$			
HMNM	δ_1, δ_3	4	$\pm 60°$, $180°$	324	283 (72)[a]	206307 (52488)[a]
	μ_2	2	$\pm 90°$			

[a] The values in parenthesis for HMNS and HMNM are N_s' and N_c after the application of screening.

using the Tripos Force Field 5.2[12]. Torsion angles for the rotational isomers that define the number of starting conformations, N_s, are summarized in the fourth column of Tab. 2.

Fig. 6 defines three types of torsional angles denoted by θ, μ and δ. Their preferred values were obtained by a search around each of the bonds in fragments of the diesters. The torsion angle θ is defined by atoms 6-1-7-8 of Fig. 6(a) and Fig. 6(b), where the rotation is around the $C^{aromatic}(1)$-$C^{carbonyl}(7)$ bond. Four energy minima at $\pm 20°$ and $180° \pm 20°$ were found. The angles μ_1 and μ_2 are defined by atoms 11-10-8-7 in Fig. 6(a) and by atoms 11-10-9-8 from Fig. 6(b), respectively. They represent the rotation around the O(8)-$C^{naphthyl}(10)$ bond and the $C^{sp^3}(9)$-$C^{aromatic}(10)$ bond, respectively. Two minima, at $\pm 90°$, were obtained for μ_1, and the minima for μ_2 are at $\pm 40°$, $\pm 90°$ and $\pm 140°$. However, due to the low torsional barriers connecting the three minima with the same sign, only two states, at $\pm 90°$, were retained for μ_2. This approximation

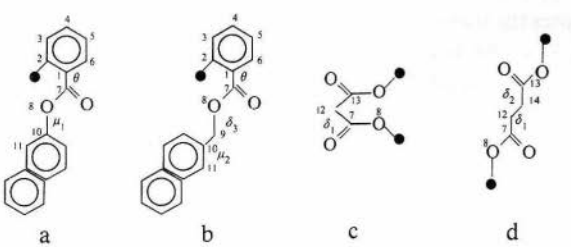

Fig. 6. Types of torsional angles found in the molecules studied

considerably reduces the number of starting conformations. The torsion angles δ_1, δ_2 and δ_3 are defined by atoms 13-12-7-8 in Fig. 6(c), 13-14-12-7 in Fig. 6(d) and 7-8-9-10 in Fig. 6(d), respectively. The rotations are around $C^{sp^3}(12)$-$C^{carbonyl}(7)$, $C^{sp^3}(12)$-$C^{sp^3}(14)$ and $O(8)$-$C^{sp^3}(9)$, respectively. Three minima, at $\pm 60°$ and 180°, were considered for δ_1, δ_2 and δ_3. Then the number of starting conformations is given by

$$N_s = \nu_\theta^{N_\theta} \nu_\delta^{N_\delta} \nu_\mu^{N_\mu} \tag{2}$$

where N_θ, N_δ and N_μ are the numbers of bonds of type θ, δ and μ found in the molecule, and ν_θ, ν_δ and ν_μ are the numbers of rotational isomers for bonds of each type. The N_s are presented in Tab. 2.

Each of the N_s conformations was optimized by using a conjugate gradient method. All atoms were used, and bond angles, bond lengths and torsional angles were variable during the minimization process. The list of optimized conformations was pruned by elimination of untenable structures and elimination of redundant copies of the same structure, as before[9]. This process reduced the number of starting conformations to N_s' (see Tab. 2) for NP, NS, NM and HMNP. For HMNS and HMNM only those optimized structures with a conformational energy within a limit of the minimum were retained. The discarded conformations were those of low probability, and their elimination represents an error of less than 0,15% in the total conformational partition function. Before the application of this additional screening, the values for N_s' and N_c — defined in the next paragraph — were 901 and 1970487, and 283 and 206307, for HMNS and HMNM, respectively, and afterwards they become 137 and 299619 for HMNS, and 72 and 52488 for HMNM.

As previously[8,9], rotatable bonds δ and μ were assigned nine orientations by allowing the preferred state and symmetric displacements from each position by an angle $\pm\Delta\phi$. The same energies were used for the preferred state and for the two symmetrically spaced partners, separated from it by $\pm\Delta\phi$, which amounts to the assumption of a square well of width $3\Delta\phi$ for each rotational isomer, and then the approximation of this square well by three equally spaced discrete torsion angles. The last column of Tab. 2 contains the number of total conformations examined, $N_c = 3^N N_s'$.

A conformational partition function, Z, was assigned to each unit as

$$Z = 3^N \sum \exp(-E_j/(RT)) \tag{3}$$

where N denotes the number of rotatable bonds to which the square well and $\Delta\phi$ were applied, and 3^N is the number of isoenergetic conformations obtained from each of the starting conformations N_s'. The summation extends over all the indistinguishable conformers, N_s'. The factor 3^N is included in the evaluation of Z because the assessment of the population of conformations conducive to a face-to-face complex evaluates

$$p_j = Z^{-1} s_j \exp(-E_j/(RT)) \tag{4}$$

$$p = \sum p_j \tag{5}$$

where s_j must be an integer from 1 to 3^N if the geometry of the aromatic rings satisfies the criteria for face-to-face complex formation, and $s_j = 0$ if none of the 3^N conformers satisfies the criteria.

For applying the criteria of intramolecular excimer formation, each phenyl group was treated separately. The three geometric parameters used previously[7-9] were measured: d_z is the shortest distance between the center of mass of a six-membered ring in one naphthalene unit and the mean plane of a six-membered ring in the other naphthalene unit, d_{xy} is the lateral offset of the two six-membered rings that define d_z, and Ψ is the angle between the normals to the mean planes of the naphthalene units. The tolerances used here, and previously[7-9], for the formation of face-to-face complexes were:

$$3{,}35 \text{ Å} < d_z < 3{,}9 \text{ Å} \qquad 0 < d_{xy} < 1{,}35 \text{ Å} \qquad 0 < \Psi < 40°$$

Types of intramolecular face-to-face complexes

The six-membered rings from each naphthalene group were named B1, B2 and B3, B4, as illustrated in Fig. 7. The carbon atoms in each naphthalene ring are labelled sequentially as 1 – 10 (and 1′ – 10′). The aromatic carbon atoms directly bonded to the ester groups are 2 (and 2′).

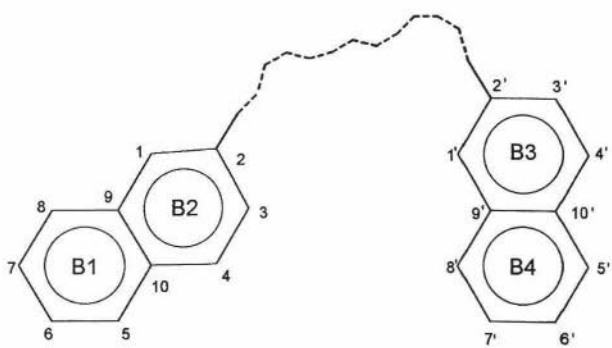

Fig. 7. Labelling of the six-membered rings and carbon atoms in the naphthalene rings

The types of intramolecular complexes formed by overlap of one ring from each of the two naphthalene units were sorted into four groups as in the previous papers[13,14], using dihedral angles defined by carbon atoms 9-6...10′-2′, 9-6...6′-9′, 2-10...10′-2′ and 2-10...6′-9′ from both naphthalene units. The terminology used[13,14] for the different geometries of face-to-face complexes is eclipsed, ortho, meta and para. These complexes, depicted in the top of Fig. 8, are defined as follows: eclipsed, $-30° < \alpha < 30°$; ortho, $30° \leq \alpha < 90°$ or $-90° < \alpha \leq -30°$; meta, $90° \leq \alpha < 150°$ and $-90° \leq \alpha < -150°$; para, $-150° \leq \alpha \leq 150°$, where α denotes the appropriate dihedral angle. There are also two possible interactions, (1) B2-B3 and B1-B4 or (2) B2-B4 and B1-B3, where both rings from one naphthalene overlap the two rings from the other

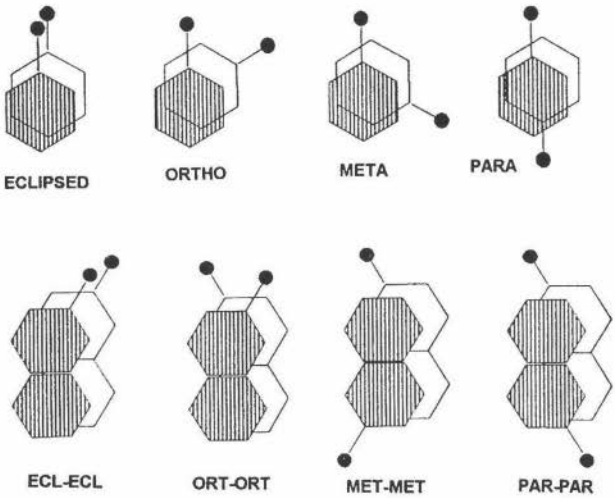

Fig. 8. Classification of the types of complexes that might be formed by overlap of one or two rings

naphthalene. These complexes were classified as eclipsed-eclipsed, ortho-ortho, meta-meta and para-para, according to the simultaneous overlap of the six-membered rings of each naphthalene group. The bottom of Fig. 8 depicts these types of face-to-face complexes.

Theoretical results

Tab. 3 shows the theoretical expectation for the probabilities for the different types of face-to-face complexes for the six compounds. According to these results, only the compounds derived from HMN, i. e., HMNP, HMNS and HMNM, have probabilities different from zero. The probabilities obtained from the calculation are zero for NP, NM and NS, which is consistent with the experimental behavior.

Tab. 3. Probabilities for the face-to-face complexes [a)]

Compound	Eclipsed (eclipsed-eclipsed)	Ortho (ortho-ortho)	Meta (meta-meta)	Para (para-para)	Total (total)
NP, NS, NM	0	0	0	0	0
HMNP	0	0,000141	0	0	0,000141
	(0,000142)	(0,000438)	(0)	(0)	(0,000580)
HMNS	0,00165	0,00872	0,000598	0	0,0126
	(0,000107)	(0,00316)	(0)	(0)	(0,00327)
HMNM	0,0153	0,00918	0	0	0,0245
	(0,00309)	(0,00609)	(0)	(0)	(0,00918)

[a)] Values outside (inside) parenthesis are for complexes with one (two) pairs of overlapping rings. For all complexes with one pair of overlapping rings, these rings are B2 and B3.

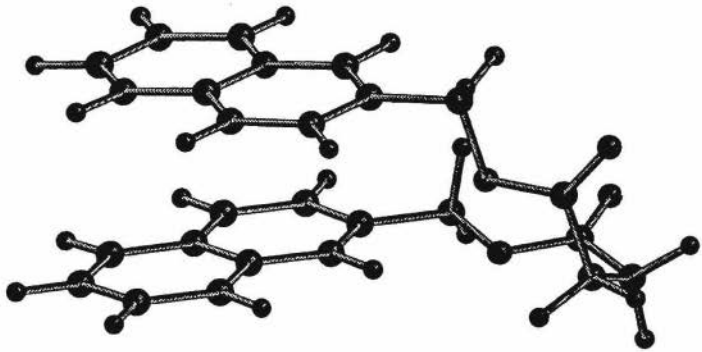

Fig. 9. A conformation of HMNS with an overlap of the ortho type. Torsional angles are 14,5°, −174,0°, −39,7°, −50,2°, 93,1°, −177,7° and −96,5°, d_z = 3,30 Å and Ψ = 2,16°

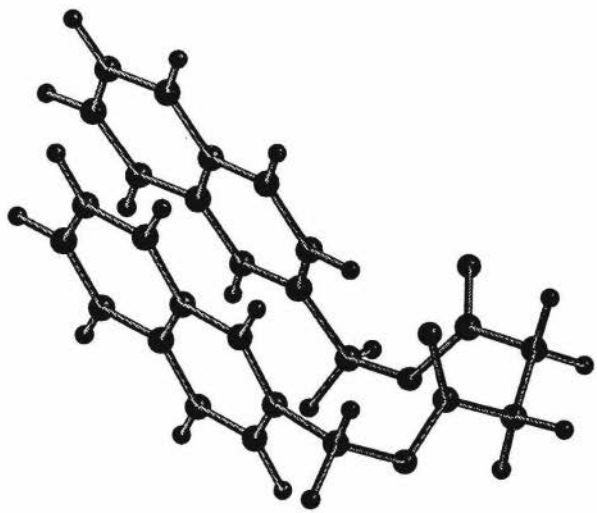

Fig. 10. A conformation of HMNS with an overlap of the ortho-ortho type. Torsional angles are −129,8°, 67,7°, 153,0°, −59,8°, −14,3°, −67,2° and 176,7°, d_z = 3,67 Å and Ψ = 2,37°

Face-to-face complexes formed by interaction of one ring from each of the two naphthalene units (B2-B3) in HMNP, HMNM and HMNS are mainly of the eclipsed and ortho types. In the complexes formed by overlap of two rings from each naphthalene unit of HMNP, HMNM and HMNS, the interactions were between rings B2-B3 and B1-B4. Figs. 9 and 10 depict conformations of HMNS with overlaps of one and two pairs of rings, respectively. The total probabilities, considering the one- and two-rings complexes, are in the order HMNM > HMNS > HMNP, which is also the order of the I_D/I_M in Fig. 5.

This research was supported by *DGICYT PB91-0166* (FM) and by *National Science Foundation grant DMR 9220369* (WLM).

[1] J. Guillet, *"Polymer Photochemistry and Photophysics"*, Cambridge University Press, Cambridge 1985
[2] F. Mendicuti, B. Patel, W. L. Mattice, *Polymer* **31**, 453 (1990)
[3] F. Mendicuti, B. Patel, W. L. Mattice, *Polymer* **31**, 1877 (1990)
[4] F. Mendicuti, E. Saiz, I. Zúñiga, B. Patel, W. L. Mattice, *Polymer* **33**, 2031 (1992)
[5] F. Mendicuti, E. Saiz, W. L. Mattice, *Polymer* **33**, 4908 (1992)
[6] J. Gallego, F. Mendicuti, E. Saiz, W. L. Mattice, *Polymer* **34**, 2475 (1993)
[7] J. Bravo, F. Mendicuti, W. L. Mattice, *J. Polym. Sci., Part B: Polym. Phys.* **32**, 1511 (1994)
[8] F. Mendicuti, W. L. Mattice, *Polymer* **33**, 4180 (1992)
[9] F. Mendicuti, W. L. Mattice, *Comput. Polym. Sci.* **3**, 131 (1993)
[10] F. Hirayama, *J. Chem. Phys.* **42**, 3163 (1963)
[11] D. D. Perrin, W. L. F. Armarego, D. R. Perrin, *"Purification of Laboratory Chemicals"*, Pergamon Press, New York 1966, p. 110
[12] M. Clark, R. C. Cramer III, N. Van Opdenbosch, *J. Comput. Chem.* **10**, 982 (1989)
[13] F. Mendicuti, W. L. Mattice, *Comput. Polym. Sci.* **2**, 203 (1992)
[14] J. Gallego, F. Mendicuti, W. L. Mattice, *Comput. Polym. Sci.* **4**, 7 (1994)